The Journal of Physiology

Heartbeat-related activity in the anterior thalamus differs between phasic and tonic REM sleep

Péter Simor[1,2], Róka Zita Lilla[1,3], Orsolya Szalárdy[2], Zsófia Jordán[4], László Halász[4], Loránd Erőss[4], Dániel Fabó[4] and Róbert Bódizs[2]

[1]*Institute of Psychology, ELTE, Eötvös Loránd University, Budapest, Hungary*
[2]*Institute of Behavioural Sciences, Semmelweis University, Budapest, Hungary*
[3]*HUN-REN Institute for Computer Science and Control, Budapest, Hungary*
[4]*Department of Neurosurgery, Faculty of Medicine, Semmelweis University, Budapest, Hungary*

Handling Editors: Richard Carson & Diana Martinez

The peer review history is available in the Supporting Information section of this article (https://doi.org/10.1113/JP287802#support-information-section).

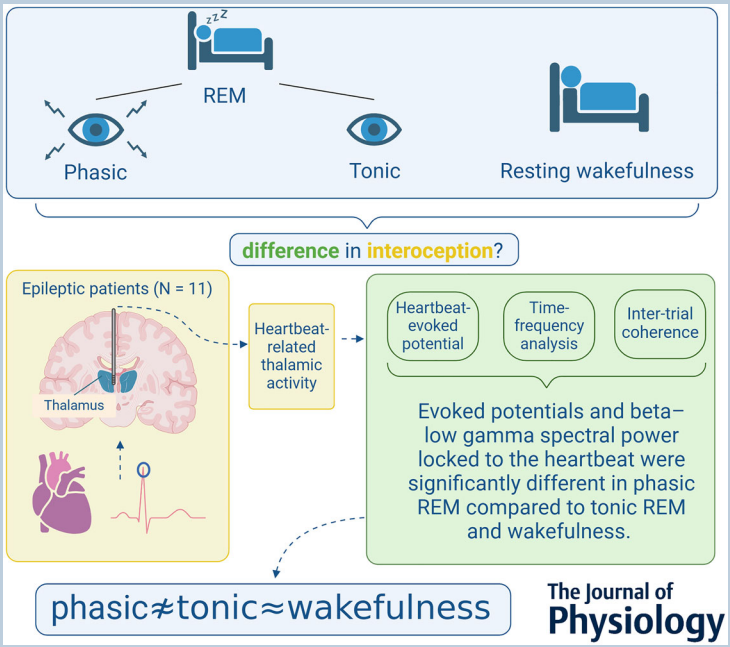

Abstract figure legend Periods of rapid eye movement (REM) sleep with or without ocular activity (phasic and tonic REM, respectively), as well as quiet wakefulness of comparable duration were contrasted in terms of interoceptive processing at the thalamic level. Eleven epilepsy patients involved in an anterior thalamus (ANT) deep brain stimulation (DBS) protocol undergoing thalamic local field potential (LFP) recordings by reliance on externalized DBS leads and co-registration of scalp EEG and ECG were involved in the study. R-peaks of the ECG were semi-automatically detected and heartbeat-related ANT activity was analysed in terms of the heartbeat-evoked potential, time-frequency measures and inter-trial coherence values. Findings reveal several significant contrasts between phasic and tonic REM sleep, as well as between phasic REM sleep and wakefulness, but not between tonic REM sleep and wakefulness, indicating a notable attenuation of interoceptive processing in the human ANT associated with ocular activity in REM sleep.

This article was first published as a preprint. Simor P, Zita Lilla R, Szalárdy O, Jordán Z, Halász L, Erőss L, Fabó D, Bódizs R. 2024. Heartbeat related activity in the anterior thalamus differs between phasic and tonic REM sleep periods. bioRxiv. https://doi.org/10.1101/2024.09.30.615986

DOI: 10.1113/JP287802

Abstract Rapid eye movement (REM) sleep is a fundamental sleep state associated with diverse functions from elemental physiological processes to higher order neurocognitive functions. A growing body of research indicates that REM sleep with eye movements (phasic REM) differs from REM periods without ocular activity (tonic) in terms of spontaneous and evoked neural responses. Studies using auditory stimulation consistently observed enhanced evoked responses in tonic *versus* phasic REM, indicating that external processing is largely diminished when the eyes move during REM sleep. Whereas exteroceptive processing during sleep is widely studied, investigations on interoception (the processing of bodily signals) during sleep are scarce, and limited to scalp electroencephalographic recordings. Here we studied interoceptive processing in a group of epileptic patients ($N = 11$) by measuring their heartbeat-related neural activity in the anterior nuclei of the thalamus (ANT) during phasic and tonic REM sleep and resting wakefulness. Evoked potentials and beta–low gamma spectral power locked to the heartbeat were significantly different in phasic REM compared with tonic REM and wakefulness. Heartbeat-related neural signals exhibited pronounced inter-trial phase synchronization at lower (7–20 Hz) oscillatory activity in all vigilance states, but reduced gamma synchronization at later time points in phasic REM only. Tonic REM and wakefulness did not show significant differences in heartbeat-related activity in the ANT. Our findings indicate that heartbeat-related neural activity is detectable at the level of the ANT, showing distinct signatures of interoceptive processing in phasic REM compared with tonic REM and wakefulness.

(Received 3 October 2024; accepted after revision 24 March 2025; first published online 14 April 2025)
Corresponding author Róbert Bódizs: Institute of Behavioural Sciences, Semmelweis University, Budapest, Hungary. Email: bodizs.robert@semmelweis.hu

Key points

- We studied interoceptive processing in the anterior the thalamus (ANT).
- The ANT tracks cardiac signals during wakefulness and rapid eye movement (REM) sleep.
- Phasic REM shows distinct patterns of heartbeat-related oscillatory activity.
- Interoceptive processing might be attenuated during REM periods with eye movements.

Introduction

Rapid eye movement (REM) is a fundamental sleep state that occupies around 20% of the total sleep time in human adults (Blumberg et al., 2022) and seems to play prominent roles in various biological functions including neurodevelopment, synaptogenesis and neural pruning, as well as cognition and affect (Blumberg et al., 2022, 2020; Li et al., 2017). Compared with non-REM sleep, REM sleep is characterized by mostly low-amplitude, high-frequency EEG activity, alongside the transient appearance of slower frequency activities (such as bursts of 1–4 Hz delta waves and 4–7 Hz sawtooth waves). Additionally, irregularities in respiration and heartbeat are common during REM sleep (Blumberg et al., 2020). The combination of intense cortical and mental (dream) activity with muscular atonia makes this state appear peculiar, which is why it was also named paradoxical sleep (Jouvet, 1965). REM sleep features the alternation of periods with and without rapid ocular activity, often referred to as phasic and tonic REM states (Simor et al., 2020). Periods of rapid eye movements (phasic REM)

Péter Simor is a psychologist with a particular interest in the neuroscience of sleep, dreaming and mind-wandering. He is Associate Professor at Eötvös Loránd University (Budapest) and head of the Budapest Laboratory of Sleep and Cognition where he investigates a diverse range of topics related to sleep and dreaming, such as the neurophysiology of paradoxical (REM) sleep, the interplay between sleep and mental health, and the links between mind-wandering and information processing. Being an expert in cognitive neuroscience and sleep EEG, he applies a variety of methods to study the sleeping brain in healthy and pathological conditions.

are linked to neural activity originating from the pons (laterodorsal peduncolopintine tegmental nuclei) and propagating to the cortex (Fernández-Mendoza et al., 2009). However, phasic REM may also be initiated from top-down cortical projections extending to deeper regions (cortico-hypothalamic projections) (Hong et al., 2023).

Phasic and tonic REM periods alternate approximately every 60–70 s in humans (Bueno-Junior et al., 2023), and are proposed to represent two core aspects of sleep: environmental disconnection during phasic and external monitoring during tonic REM (Simor et al., 2020). Evidence supporting the distinct roles of phasic and tonic REM periods comes from studies aiming to probe cortical reactivity to external stimulation during REM sleep. These findings indicate that arousal and awakening thresholds are lower in tonic than phasic REM, the latter even reaching levels of the deepest stage of NREM sleep (Ermis et al., 2010). Moreover, acoustic stimuli during REM sleep appeared to elicit heightened cortical responses in tonic *versus* phasic REM sleep, suggesting that sensory information arriving from the external environment is selectively suppressed when the eyes move during REM sleep (Koroma et al., 2020; Takahara et al., 2006). Attenuated reactivity to sensory stimulation during phasic REM was also corroborated in an fMRI study that examined whole-brain blood oxygen level dependent responses in REM sleep under acoustic stimulation (Wehrle et al., 2007). Whereas residual activity in auditory processing regions during tonic REM sleep were elicited to some extent and resembled those observed during resting wakefulness, in phasic REM periods no such responses were apparent. On the other hand, phasic REM featured the activity of a widespread thalamocortical network which appeared to be functionally isolated from external stimulation (Wehrle et al., 2007).

Reactivity to environmental stimuli during sleep is not limited to external sensory inputs. The perception of the internal state of the body through diverse (e.g. chemical, somatosensory, visceral, or neural) ascending pathways, known as interoception, is critical to generate the cortical representation of the body, which in turn functions as an interface between the brain and the body to adaptively regulate homeostatic functions, as well as to contribute to motivated behaviour and affective states (Feldman et al., 2024; Seth, 2013). Although our sense of our body seems to be lost when we fall asleep, empirical studies indicate that interoceptive processing is maintained by the sleeping brain to some extent (Mazza et al., 2012; Wei & Van Someren, 2020), and seems to influence the regulation of sleep and arousal (Bastuji et al., 2008). Heartbeat-related cortical activity is one of the most studied measures of interoceptive processing (Coll et al., 2021). Cortical responses locked to the R-peak of the heartbeats vary in different states of vigilance and arousal, and also across phasic and tonic REM sleep (Immanuel et al., 2014; Simor, Bogdány et al., 2021). More specifically, heartbeat-related potentials measured at the level of the scalp were not different in tonic REM and resting wakefulness but differed in phasic REM periods at late ($\sim$ 500 ms after the R-peak) components (Simor, Bogdány et al., 2021).

Although heartbeat-related cortical activity is a widely used measure of interoceptive processing, only a few studies assessed heartbeat-related activity beyond the level of the scalp (Park et al., 2018). Nevertheless, the processing and integration of bodily signals relies on extended subcortical pathways involving structures lying deep below the scalp such as the nucleus of the solitary tract, the parabrachial nucleus and the periaqueductal grey, to reach multimodal cortical sites such as the insula, and fronto-limbic regions through the thalamus (Berntson & Khalsa, 2021; Feldman et al., 2024; Park & Blanke, 2019).

Here, we studied heartbeat-related activity in REM sleep and resting wakefulness by assessing local field potentials (LFPs) of the anterior nuclei of the thalamus (ANT) in a group of epileptic patients undergoing surgery for deep brain stimulation (DBS). The ANT, being a key hub of the limbic system, is assumed to be involved in the integration and regulation of autonomic (visceral) inputs through its involvement in hippocampal–diencephalic and parahippocampal–retrosplenial networks (Child & Benarroch, 2013; Gonzalo-Ruiz et al., 1995; Grodd et al., 2020; Vertes et al., 2001). Animal data also indicate that the ANT, especially the anterodorsal portion, influences the hypothalamic–pituitary–adrenal axis under stressful conditions (Suarez et al., 1998). Moreover, a more recent study found that DBS of the ANT in epileptic patients increased heart rate variability (Lőrincz et al., 2023), indicating a potentially positive influence on autonomic regulation. Moreover, as part of the fronto-limbic network, the ANT is intimately linked to brain regions (e.g. amygdala, ventromedial prefrontal and anterior cingulate cortex) that orchestrate REM sleep (Hasegawa et al., 2022; Luppi et al., 2011; Miyauchi et al., 2009) and are also involved in the integration of interoceptive signals (Boccia et al., 2023; Feldman et al., 2024; Pollatos et al., 2007), making it a suitable diencephalic site below the cortex to study heartbeat-related activity in different vigilance states. In line with the notion of phasic REM as a state of environmental disconnection which also involves interoceptive processing, we expected distinct heartbeat-related neural responses in the ANT in phasic REM compared with tonic REM and wakefulness.

Methods

Ethical approval

The study protocol was approved by the local ethical committee of the National Institute of Clinical Neuro-

sciences (Intézeti Kutatásetikai Bizottság, IKEB 6/2016), and all patients were provided with written informed consent according to the ICH – GCP and the *Declaration of Helsinki*. The study conformed to the principles of the *Declaration of Helsinki*, except for registration in a public database.

Participants

We examined the data from 12 epilepsy patients (mean age = 35.33 years; SD = 13.03; range: 17–64 years; 7 females) who were undergoing ANT DBS treatment at the National Institute of Clinical Neurosciences in Budapest, Hungary. Patients were selected from a larger pool (N = 20) based on the following inclusion criteria: one (seizure- and stimulation-free) recording night of co-registered ANT LFPs and ECG was available, along with sufficient amounts (at least 5 min) of both phasic and tonic REM sleep segments in their nocturnal recordings, and a similar amount of awake resting state recordings. One patient was excluded due to a noisy ECG signal hindering the analyses of heartbeat-related activity. Clinical and demographic data are reported in Table 1.

Surgical procedures

Medtronic DBS electrodes were stereotactically implanted bilaterally in the anterior thalamus under general anaesthesia to mitigate seizures in pharmacoresistant, surgically untreatable epilepsy patients. In addition to mostly frontal transventricular trajectories (nine patients), extraventricular trajectories and posterior parietal extraventricular approaches were employed based on the decisions of the clinical-neurosurgical team.

Localization of ANT channels

Preoperative MRI and postoperative CT images were co-registered using tools from the FMRIB Software Library (FSL, Oxford, FLIRT, linear registration, 6 degrees of freedom) to ensure precise localization of thalamic contacts. A threshold was applied to the co-registered CT scans to achieve the desired density for proper lead identification, thus excluding the surrounding brain tissue. The coordinates of the lead's most distal point were identified, and a more proximal point was selected along the line of contacts to mathematically reconstruct the centre point coordinates of each contact using Euclidean distance in three-dimensional space. These points, superimposed on the T1 MRI image, provided a guideline for contact localization by examining their position relative to the anatomical boundaries of the ANT (see Simor, Szalárdy et al. (2021) for more details). The anatomical positions of the contacts were double-checked using the mamillothalamic tract as a guide to localize the ANT. When both methods produced convergent results, the ANT contacts were considered suitable for further analyses.

Electrophysiological recordings

Externalized DBS electrodes were connected to an EEG headbox/amplifier. Electrophysiological and video recordings were performed by using an SD-LTM 64 Express EEG/polygraphic recording system and the System Plus Evolution software (Micromed). Signals were recorded at an 8192 Hz/channel effective sampling rate with 22-bit precision and hardware input filters set at 0.02 (high pass: 40 dB/decade) and 450 Hz (low pass: 40 dB/decade). Data were decimated by a factor of four by the firmware resulting in stored time series digitized at 2048 Hz/channel with the exception of one patient where it was set to 1024 Hz/channel due to technical issues. LFPs of the ANT were assessed by bilateral (L, left; R, right) quadripolar electrodes (LTh0, LTh1, LTh2, LTh3, RTh8, RTh9, RTh10, RTh11) according to a bipolar reference scheme: LTh0-LTh1, LTh1-LTh2, LTh2-LTh3, LTh0-LTh3, RTh8-RTh9, RTh9-RTh10, RTh10-RTh11, RTh8-RTh11. LTh0-LTh3 and RTh8-RTh11 were the distant reference derivations on the left and the right side of the ANT, respectively. Scalp EEG allowing sleep staging was recorded following standard protocols (Keil et al., 2014). Scalp EEG was recorded at electrode placements according to the 10–20 system (Fp1, Fp2, Fpz, F3, F4, F7, F8, C3, C4, T3, T4, T5, T6, P3, P4, O1, O2, Oz) extended with the inferior temporal chain (F9, F10, T9, T10, P9, P10) and additional two anterior zygomatic electrodes (ZA1, ZA2; Manzano et al., 1986). EEG signals were re-referenced offline to the mathematically linked T9 and T10 points [(T9 + T10)/2]. Ocular movements facilitating the identification of phasic and tonic segments were assessed by the ZA1-ZA2 bipolar record created by offline re-referencing. Submental EMGs were recorded by bipolarly referenced electrodes placed on the chin. ECG activity was recorded by an electrode placed at the mid-clavicular line on the left and the fifth intercostal space referred to the CP1 location on the scalp.

Data preprocessing

Data and statistical analyses were performed in MATLAB, using custom-based scripts and functions from the Fieldtrip toolbox (Oostenveld et al., 2011) and in JASP (0.18.3) (Team 2020). Acquisition of stimulation-free nocturnal recordings after the surgical implantation of thalamic contacts has previously been described in detail (Simor, Szalárdy et al., 2021; Szalárdy et al., 2024). In sum, continuous EEG and LFP recordings were segmented into

Table 1. Clinical data of the subjects involved in the study.

Pat.	Onset of epilepsy (age)	Years since epilepsy onset	Aetiology	Epilepsy syndrome	Highest phase of epilepsy evaluation	Earlier surgical interventions	Seizures/ month before DBS	Medication (daily dose in mg)
#1	34	30	postencephalitis/ negative MRI	bitemp.	Phase II- FO	-	12—14	lacosamide 400, lamotrigine 400, oxcarbamazepine 600
#2	12	5	unknown	bitemp.	Phase II- FO, Strip	-	12	carbamazepine CR 800, lamotrigine 300, clonazepam 0.5, clobasam 20, quetiapine 50
#3	19	16	postencephalitis/ negative MRI	left fronto-temporal	Phase II- Strip + Grid	left temporal resection, VNS	6–10	clonazepam 2, lamotrigine 425, phenobarbital 100, risperidone 2.5
#4	19	7	bilat. PVNH	bitemp.	Phase I	-	2	oxcarbamazepine 1800, levetiracetam 2000, topiramate 300, sulthiam 300
#5	12	34	assumed HS	bitemp.	Phase II- FO	right temporal resection	2–4	clobasam 20, oxcarbamazepine 600, lacosamide 400, topiramate 200
#6	2	38	unknown	multifocal fronto-temporal	Phase II- Strip	-	2–4	zonisamide 300, lamotrigine 250
#7	18	18	bilat. parietal polymicrogyria, bilat. HS	bitemp.	Phase II- FO	VNS	14–20	levetiracetam 3000, carbamazepine 1500, zonisamide 400
#8	15	23	left HS	bitemp.	Phase II- FO	-	4–5	carbamazepine CR 700, clobazam 20, zonisamide 200
#9	23	18	uncertain HS with left dominance	bitemp.	Phase II- FO	-	2–3	lacosamide 300, levetiracetam 1500
#10	12	13	bilateral HS	Bitemp	Phase II- FO	VNS	20–30	levetiracetam 3000, lamotrigine 400
#11	17	25	left temporal dysgenesis/ peritrigonal heterotopia	left fronto-temporal	Phase I	left temporal resection 2×, peritrigonal heterotopia resection	4–5	lacosamide 500, gabapentin 1200, alprazolam 1, perampanel 10 mg

bitemp – bitemporal; FO – foramen ovale electrodes; CR – controlled release; HS – hippocampal sclerosis; PVNH – periventricular nodular heterotopia; VNS – vagus nerve stimulation; DBS – deep brain stimulation; Phase I – video-EEG monitoring with scalp electrodes; Phase II –video-EEG with invasive electrodes.

Table 2. Sleep architecture of the night records of the subjects involved in the study (all measures are expressed in minutes).

Patient	Total recording time	TST	WASO	Wake	Stage1	Stage2	Stage3	REM	Phasic REM #	Tonic REM #	Resting wake #
#1	690.3	416	187	274.6	59.3	226.7	38.7	91.3	252	191	407
#2	596	542.3	29.6	53.7	45.3	312	66.7	118.3	118	337	205
#3	662.6	247.7	92.3	415	62	146.3	0	39.3	67	83	362
#4	503	461.3	38.7	41.7	10	296.7	86	68.7	390	1263	394
#5	450	397	29.3	53	24	168	82.7	122.3	455	708	374
#6	450	347.3	76.3	102.7	26.3	274.3	14.3	32.3	113	189	148
#7	450	294.3	155.6	155.7	34	174.3	20	66	480	584	407
#8	630	522	88.7	108	19	420.7	16.7	65.7	230	1161	401
#9	720	574.3	56.7	145.7	15.7	433.3	53.3	72	744	1097	614
#10	630	493.3	119.3	136.7	25.7	386.3	36.3	45	319	782	475
#11	600	560	30	40	47	295.7	98	119.3	164	819	379

Phasic and Tonic REM and Awake trial numbers refer to the number of analysed 1 s segments locked (between -200 and 800 ms) with reference to the R-peak of the ECG signal. WASO: wake after sleep onset refers to wake time after the first epoch of not S1 sleep. TST: total sleep time. Since there were no explicit schedules of lights off, we did not analyse sleep latency and sleep efficiency.

90 min chunks by the recording software. Since there were no specific light on/off times, the first and last chunks for analysis were chosen based on containing at least 10 min of continuous sleep in the second half for the first chunk and the first half for the last chunk. REM periods following sleep staging according to standardized criteria (Berry et al., 2012) were selected for further analyses. REM periods with (phasic REM) and without (tonic REM) eye movements were identified by visual inspection using the EOG channels. All identified REM periods from the full-night recording were considered in selecting specific phasic and tonic REM segments. 4 s long segments were coded as phasic when the bipolar EOG channel exhibited at least two consecutive eye movements and featured 100 μV (or larger) amplitudes within the specific time window. 4 s long segments without significant bursts of eye movements (EOG deflections lower than 25 μV) were categorized as tonic REM. The selection of segments was conducted by research assistants trained in sleep scoring, and the selected 4 s periods were visually inspected by a trained sleep researcher to exclude segments with inaccurate categorizations. Segments with artefacts in the ANT and/or ECG channel and those showing inter-ictal spikes or signs of pathological activity were discarded after further visual inspection. To compare REM microstates with resting wakefulness, 5–10 min of segments containing eyes-closed wakefulness were selected for further analyses. Since resting state and eyes-closed recordings were limited in number in our sample, and on many occasions were contaminated by movement-related artefacts, we selected awake segments from both pre-sleep wakefulness and from periods of wake after sleep onset throughout the night. Similar to the selection of REM segments, eyes-closed, awake segments from the full-night recording were also considered. Given that many patients spent a significant amount of time awake even after sleep onset (see Table 2), the awake samples included a mix of night-time resting states, pre-sleep onset wakefulness, and intra-sleep awakenings. Since resting state recordings were limited in number in our sample, we selected awake segments from both pre-sleep wakefulness and from periods of wake after sleep onset throughout the night. Preprocessing steps of wake trials were identical to those performed on REM trials. Segments were band pass-filtered between 0.3 and 70 Hz (with Butterworth, zero phase forward and reverse digital filters) and down-sampled to 512 Hz.

R-peaks of the ECG channel were identified semi-automatically using scripts of the HEPLAB toolbox (Perakakis, 2019). Available ANT channels in each participant were segmented to epochs of 1000 ms spanning between -200 ms and +800 ms time-locked to the R-peak of the ECG channel, yielding to an average number of 302.9 trials (SD: 246.5, range: 67–744) in phasic, 655.5 trials (SD: 438.4, range: 83–1263) in tonic, and 378.7 trials (SD: 152.61, range: 148–614) in resting wakefulness. Sleep architecture and the number of selected trials for each participant are summarized in Table 2.

Data analyses

All analyses were performed in MATLAB, using custom-based scripts and functions from the Fieldtrip toolbox (Oostenveld et al., 2011).

Heartbeat-evoked potentials (HEPs) were computed from the ANT recordings. One-second trials, locked to the cardiac signal (from -200 to +800 ms relative to the

R-peak), were averaged for each condition (phasic REM, tonic REM, wake) in each participant. For participants with multiple ANT contacts ($N = 5$), polarity reversals were visually inspected and inverted before averaging over channels within participants. Averaged amplitudes locked to the heartbeat were baseline corrected with their mean amplitudes between -200 and -50 ms to avoid the influence of the rising edge of the R wave (Coll et al., 2021; Schandry et al., 1986). Amplitude fluctuations locked to the heartbeat were statistically compared between conditions along the time window between 350 and 650 ms after the R-peak. We focused on this time window because HEP-like waveforms were previously identified in REM sleep at late components (Perogamvros et al., 2019), the influence of the cardiac R and T waves might be reduced at 350 ms after the R-peak (Park & Blanke, 2019), and a previous scalp EEG study identified HEP differences between REM microstates and wakefulness also in late components (Simor, Bogdány et al., 2021). To ensure that the observed differences in HEP amplitudes were not caused by differences in ECG activity, the ECG waveforms pertaining to the selected trials were also averaged and compared across the three conditions. The aim of this approach was to control for any confounding influence of ECG activity on the observed differences in HEP across the three conditions (Park & Blanke, 2019).

We performed *time-frequency analyses (TFA)* to characterize heartbeat-related anterothalamic LFPs in more detail. Power values along the time and frequency dimensions were extracted using Fast Fourier Transformation (FFT) of overlapping, Hanning-tapered, 150 ms time windows, sliding in 10 ms steps over the selected 1 s long trials. Zero-padding was applied to extend the signal to 1.2 s before performing the FFT. Power values between 7 and 45 Hz (with 1 Hz frequency resolution) locked to the R-peak were considered for further analyses. We applied baseline correction (using the period between -200 ms and -50 ms with reference to the R-peak), and changes in power were defined relative to this baseline. The trials of time-frequency power modulations locked to the R-peak were averaged within each condition in each participant. Similarly, to the HEP analysis, the power values of participants with multiple ANT channels were averaged before statistical comparisons.

Finally, *inter-trial phase coherence (ITPC)* was computed to investigate the consistency of the phase of frequency-specific oscillatory activity relative to the heartbeat. ITPC is a measure of the phase consistency of oscillatory signals across trials and is particularly useful for examining whether oscillatory activity is phase-locked to an event; in this case, the R-peak of the heartbeat. The phase information was extracted from the same time-frequency decomposition used for the TFA, which involved applying an FFT to overlapping, Hanning-tapered, 150 ms time windows sliding in 10 ms steps across the 1 s trials. For each trial, frequency-specific phase angles were computed across the frequencies of interest (7–45 Hz with 1 Hz resolution). The padding was set to 1.2 s to avoid edge effects and to ensure accurate phase estimation. ITPC was calculated as follows:

The phase and amplitude of the signal at each frequency and time point were extracted using complex values obtained from the FFT. The phase angle ($\theta_{f,}$) at each frequency (f) and time point (t) was used for subsequent ITPC calculations. ITPC was computed as the absolute value of the average of the unit vectors representing the phase angles across trials:

$$ITPC\left(f,t\right) = \left|\frac{1}{n}\sum_{n=1}^{N} e^{i\theta_{f,t,n}}\right| \quad (1)$$

where N is the number of trials, and $\theta_{f,t,n}$ is the phase at the nth trial at frequency f and time t. This results in ITPC values ranging from 0 to 1, where 0 indicates completely random phases across trials (i.e. high variability) and 1 indicates perfect phase alignment (i.e. high consistency) (Cohen, 2014).

ITPC values were baseline-corrected (baseline between: -200 ms and -50 ms) to highlight relative changes in phase consistency with respect to heartbeats. For TFA and ITPC, statistical comparisons between conditions (phasic REM, tonic REM, wakefulness) were performed within the time range of 50 ms to 650 ms after the R-peak, as amplitude and phase modulations in intracranial recordings were observed over a broader time range also including early components (García-Cordero et al., 2017; Park et al., 2018).

Statistical analyses

Differences between conditions (phasic REM, tonic REM, wakefulness) were evaluated by pairwise comparisons using cluster-based statistics, a suitable approach for the statistical analyses of EEG data. Cluster-based permutation statistics is a non-parametric approach that neither applies degrees of freedom nor relies on assumptions of data distribution. In addition, it efficiently addresses the issue of multiple comparisons (Maris & Oostenveld, 2007). In brief, two-tailed, paired t-tests were performed contrasting each condition (i.e. phasic *vs.* tonic, phasic *vs.* wake, tonic *vs.* wake) along each data point within the time axis (in the case of HEP), and time × frequency axes (in the case of TFA and ITPC). These parametric statistical comparisons served as inputs for the non-parametric cluster-based statistics, which assess the significance of clusters of adjacent significant t-tests. Clusters were defined if at least two adjacent time points or neighbouring frequency bins showed significant differences with the degrees of freedom equal to n-1 =

10 (for $n = 11$) at the alpha level below 0.05. For each cluster, the observed cluster statistic was calculated as the sum of all t-values within the cluster. This process was repeated 2048 (2^{11}) times using Monte Carlo simulations, where conditions were randomly shuffled to generate a null distribution of the largest clusters produced by chance. (The number of permutations reflected the maximum number of simulated samples achievable by Monte Carlo simulations.) During these simulations, clusters were defined using the same criteria as in the observed data (significant adjacent bins of time points or frequency bins), but only the largest cluster from each permutation was retained for comparison. Finally, the observed cluster statistics were tested against the null distribution of maximal cluster statistics of the simulated dataset, with an alpha level of 0.05. This way, an observed cluster was deemed significant if it exceeded the 95th percentile of the largest clusters in the simulated null distribution. Effect sizes (Cohen's d) for each data point within the significant clusters were computed. Cohen's d values (reported as ranges) were provided, reflecting the minimum and maximum effect sizes across time points and/or frequency bins within each significant cluster.

Results

Anterior thalamic HEPs are different in phasic REM compared with tonic REM and wakefulness

First, we examined whether HEPs differed across the three states within the time range of interest (350–650 ms) (Fig. 1*A*,*B*). Significant positive clusters emerged when

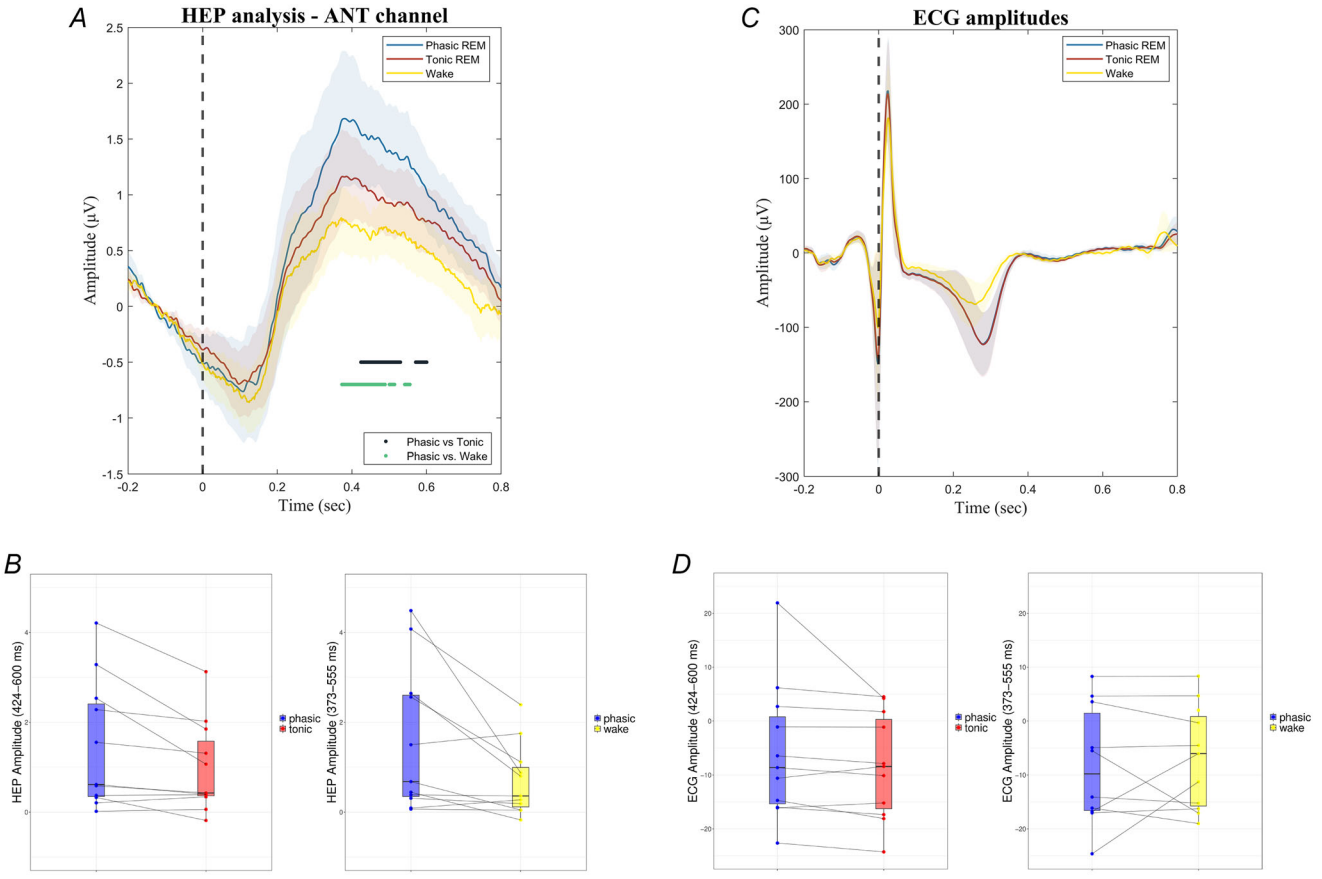

Figure 1. Heartbeat-evoked potential (HEP) in the anterior thalamus in phasic and tonic REM sleep and resting wakefulness.
A, HEP amplitudes in phasic and tonic REM and wakefulness. HEPs differed at late potentials (over ∼400 and 600 ms) between phasic REM and tonic REM, as well as between phasic REM and wakefulness. Black and green vertical lines indicate significant differences along the time axis between phasic and tonic REM, and phasic REM and wakefulness, respectively. The vertical dashed line marks the time point of the R-peak. *B*, HEP amplitudes averaged along the time ranges where significant differences emerged across conditions. *C*, averaged ECG amplitudes in the three conditions. No significant differences were observed between the three vigilance states in ECG amplitudes. *D*, ECG amplitudes averaged along the time ranges where significant HEP differences emerged between conditions. No significant differences in ECG amplitudes over the time range of interest emerged, indicating that HEP differences were not confounded by ECG activity. [Colour figure can be viewed at wileyonlinelibrary.com]

comparing phasic REM with tonic REM (424.3–529.9 ms, t_{maxsum} = 145.9478, cluster level P = 0.0151, Cohen's d = [0.68–0.95]; 571–600.4 ms, t_{maxsum} = 38.5384, cluster level P = 0.0493, Cohen's d = [0.69–0.75]) and when comparing phasic REM with wakefulness (373.4–488.8 ms, t_{maxsum} = 144.2944, cluster level P = 0.0122, Cohen's d = [0.69–0.83]; 500.6–514.3 ms, t_{maxsum} = 19.5978, cluster level P = 0.0474, Cohen's d = [0.67–0.70]; 541.7–555.4 ms, t_{maxsum} = 18.2176, cluster level P = 0.0474, Cohen's d = [0.69–0.77]). However, no significant clusters were observed when contrasting HEPs between tonic REM and wakefulness.

To control for potential confounding effects of cardiac activity, we conducted pairwise comparisons of ECG amplitudes between phasic and tonic REM, as well as between phasic REM and wakefulness, within the same time range (350–650 ms)). We also examined whether mean ECG amplitudes differed in the specific time ranges where significant HEP clusters were observed. The ECG amplitudes did not significantly differ between phasic and tonic REM ($t(10)$ = 1.518, P = 0.160, Cohen's d = 0.46) or between phasic REM and wakefulness ($t(10)$ = 0.606, P = 0.558, Cohen's d = 0.18) during these periods (see Fig. 1*D*). Additionally, no significant ECG amplitude clusters were found across conditions between 350 and 650 ms (Fig. 1*C*). These analyses suggest that HEPs in the ANT during phasic REM periods differ significantly from those during tonic REM and resting wakefulness (see Fig. 1).

Reduced heartbeat-related anterior thalamic fast frequency power in phasic REM

Next, we explored power changes relative to the R-peak and examined time × frequency power modulations across the three conditions. Similarly to HEPs, significant clusters were observed between phasic and tonic REM (time range: 315.1–444.2 ms, frequency range: 18.3–35 Hz, t_{maxsum} = -409.3936, cluster level P = 0.036, Cohen's d = [0.67–2.16]), and between phasic REM and wakefulness (time range: 164.4–465.8 ms, frequency range: 19.2–45 Hz, t_{maxsum} = -1276.6199, cluster level P = 0.002, Cohen's d = [0.67–2.24] and time range: 524.5–634.1 ms, frequency range: 28.3–45 Hz, t_{maxsum} = -322.3900, cluster level P = 0.048, Cohen's d = [0.67–1.18]), while the comparison between tonic REM and wakefulness did not yield significant clusters. As shown in Fig. 2, fast frequency activity in the beta and low gamma range (~20–40 Hz) locked to the R-peak was relatively reduced in phasic REM as compared

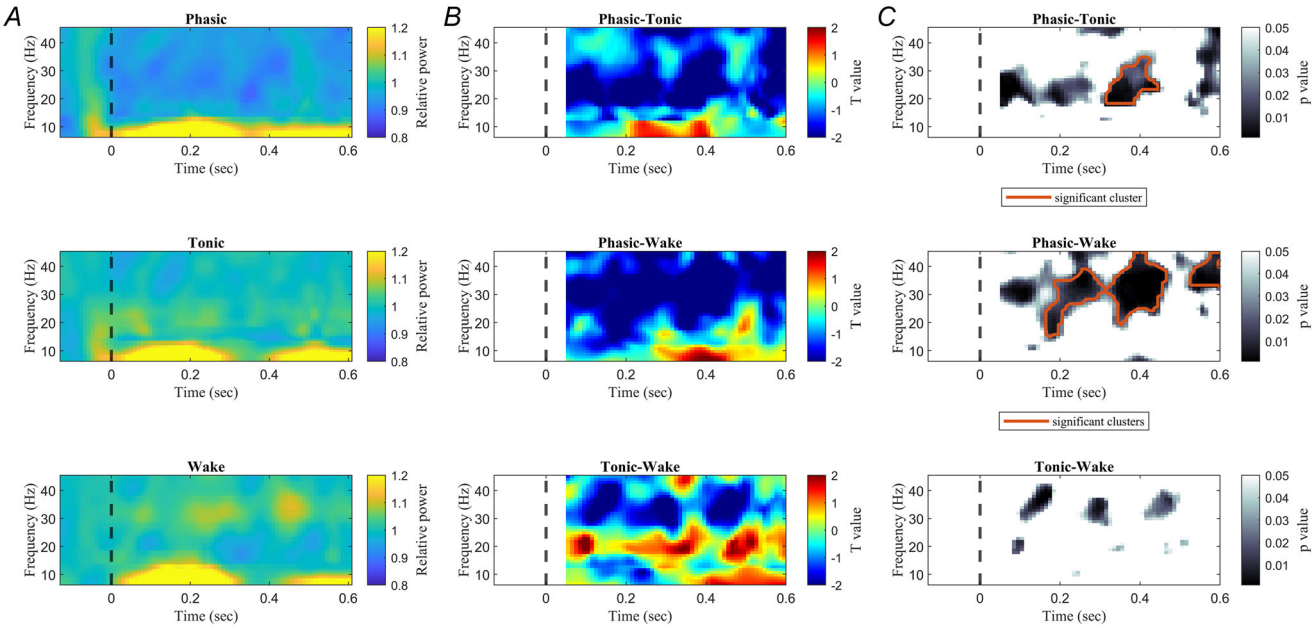

Figure 2. Power modulations in the anterior thalamus locked to the R-peak of the ECG signal.
A, changes in time-frequency power relative to the baseline period (between -200 and -50 ms) are visualized for phasic REM, tonic REM, and wakefulness. Values above 1 indicate increased power, whereas values below 1 mean reductions in power relative to the baseline. *B*, pairwise statistical comparisons across conditions highlighting the value of the statistical test (*T* value) along the time and frequency axis. *C*, uncorrected significant differences (P < 0.05) at each time × frequency point and significant clusters remaining after the correction for multiple comparisons are visualized (with red contour). Power changes locked to the R-peak in the beta and low gamma range (~20–40 Hz) were relatively reduced in phasic REM as compared with wakefulness and tonic REM sleep. The vertical dashed line marks the time point of the R-peak. [Colour figure can be viewed at wileyonlinelibrary.com]

with wakefulness and tonic REM sleep. Although fast frequency power modulation locked to the R-peak seemed to peak at relatively higher frequencies in wakefulness (above 30 Hz) than in tonic REM (between 20 and 30 Hz), these differences were not significant after cluster-based correction.

To explore whether differences across conditions in heartbeat-related high-frequency activity were mainly driven by a relative reduction of beta–low gamma power in phasic REM, or a relative increase in high-frequency power in tonic REM and wake, we contrasted power values of the baseline periods with those of the periods after the R-peak within each condition. To test whether power in the beta and low gamma (20–40 Hz) frequency range differed between the baseline (-200 ms to -50 ms) and the post-R-peak periods, we contrasted the 150 ms baseline (pre-R-peak) periods with the subsequent period after the R-peak chunked into four non-overlapping 150 ms segments between 50 and 650 ms. Fast (20–40 Hz) frequency power in the baseline periods was hence compared with the post-R-peak period using cluster-based permutations statistics along the time axis. High-frequency power fluctuations as referenced to the baseline (pre-R-peak period) were relatively reduced in phasic REM, but not in tonic REM and wakefulness. Statistically significant differences between the baseline and post-R-peak periods were only observed in phasic REM (time range: 324.8–354.2 ms, t_{maxsum} = -9.7095, cluster level P = 0.0068 Cohen's d = [0.67–1.03] and time range: 375.7–434.4 ms, t_{maxsum} = -20.9739, cluster level P = 0.0020, Cohen's d = [0.69–0.97] and time range: 565.5–575.3 ms, t_{maxsum} = -5.3738, cluster level P = 0.0283, Cohen's d = [0.59–0.77]), but not in tonic REM and wakefulness.

Heartbeat-related low-frequency phase modulation in the anterior thalamus across all vigilance states

Pairwise comparisons of ITPC between REM microstates and wakefulness are presented in Fig. 3. As indicated in the figure, no significant differences emerged between conditions after cluster-based correction of multiple comparisons. On an exploratory level, uncorrected t-tests showed trend-like differences between phasic and tonic REM microstates, showing increased ITPC in lower (∼10–17 Hz) and gamma (∼40–45 Hz) frequencies during tonic REM, and relatively increased phase coherence in the beta (∼20–30 Hz) frequency range during phasic REM. Nominal differences between phasic REM and wakefulness showed a similar pattern with respect to the relative increase in 20–30 Hz ITPC in phasic REM, and the relative increase in 40–45 Hz

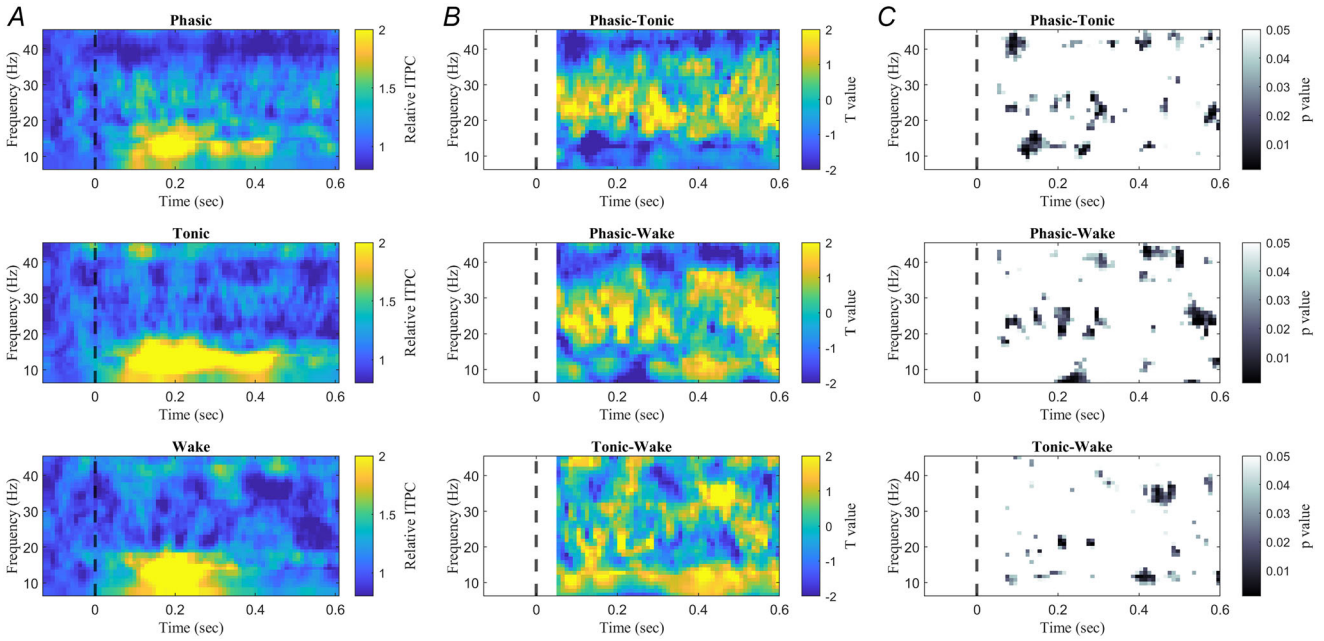

Figure 3. Inter-trial phase coherence (ITPC) in the anterior thalamus relative to the R-peak of the ECG signal.
A, changes in ITPC relative to the baseline period (between -200 and -50 ms) are visualized for phasic REM, tonic REM and wakefulness. Values above 1 indicate increased power, whereas values below 1 mean reductions in power relative to the baseline. *B*, pairwise statistical comparisons of ITPC changes across conditions highlighting the value of the statistical test (*T* value) along the time and frequency axis. *C*, uncorrected significant differences ($P < 0.05$) at each time × frequency point are visualized. Changes in ITPC locked to the R-peak were not significantly different across conditions. [Colour figure can be viewed at wileyonlinelibrary.com]

gamma ITPC in wakefulness. ITPC in tonic REM showed slightly increased values in the (8–15 Hz) alpha frequency range compared with wakefulness. Nevertheless, none of the above differences remained significant after correction for multiple comparisons.

Given that ITPC analyses indicated a robust heartbeat-related increase in low-frequency phase coherence between 7 and 20 Hz in all of the conditions (see Fig. 3), we examined whether such increase was statistically significant as compared with ITPC values of the baseline (pre-R-peak) period. Therefore, ITPC values at baseline (from -200 ms to -50 ms) were statistically compared (applying cluster-based permutation statistics) with post-R periods chunked into four non-overlapping 150 ms segments between 50 and 650 ms. ITPC between ∼7–20 Hz showed robust increases in all conditions after the R-peak between 130–444 ms in phasic REM ($t_{\text{maxsum range}}$: 182–233, cluster level $P_{\text{range:}}$ 0.0001–0.01, Cohen's d = [0.70–1.97]), between 54 and 444 ms in tonic REM ($t_{\text{maxsum range}}$: 139–258, cluster level $P_{\text{range:}}$ 0.001–0.03, Cohen's d = [0.70–1.8]), and between 55 and 424 ms in wakefulness ($t_{\text{maxsum range}}$: 139–258, cluster level $P_{\text{range:}}$ 0.001–0.03, Cohen's d = [0.70–1.80]) (Fig. 4). In addition, a negative cluster emerged in phasic REM, pointing to decreased ITPC at 36–45 Hz between 475 and 524 ms after the R-peak (t_{maxsum} = -81.1285, cluster level P = 0.0107, Cohen's d = [0.54–0.92]).

Discussion

We studied interoceptive processing during REM sleep and resting wakefulness by measuring LFP in the ANT locked to the heartbeat. Heartbeat-related neural activity in the ANT was distinct during REM periods with ocular activity (phasic REM) compared with tonic REM and wakefulness. More specifically, evoked potentials and power fluctuations of beta–low gamma frequencies locked to the heartbeat were significantly different in phasic REM states compared with tonic REM and wakefulness. On the other hand, heartbeat-related amplitude and power fluctuations did not show significant differences between tonic REM and wakefulness. Moreover, heartbeat-related neural signals exhibited pronounced phase synchronization at lower (7–20 Hz) oscillatory activity in the ANT lasting 400 ms after the R-peak in all vigilance states, but reduced gamma synchronization at later time points (∼500 ms after the R-peak) in phasic REM only. Our findings indicate that heartbeat-related neural activity is detectable at the level

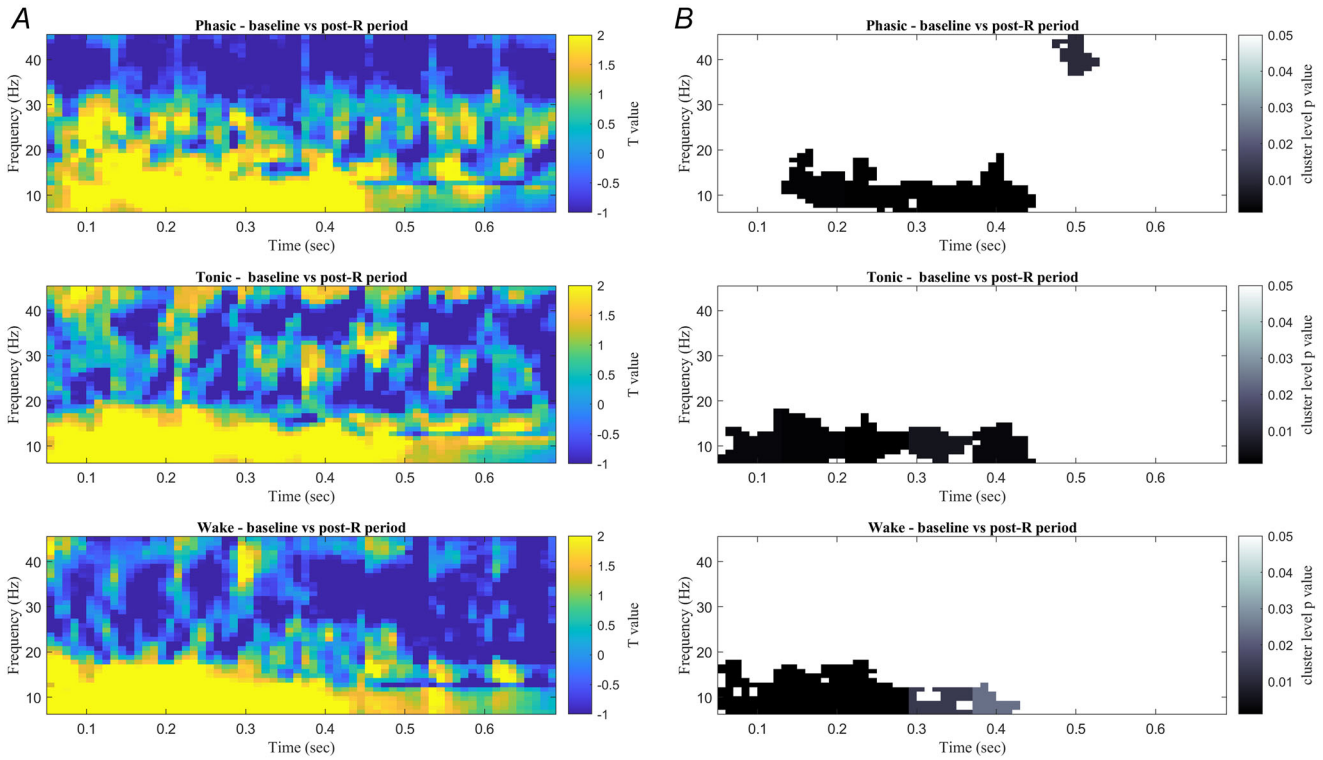

Figure 4. Changes in inter-trial coherence (ITPC) in the anterior thalamus locked to the R-peak.
A, statistical comparisons of ITPC between the baseline period (-200–-50 ms) and the post-baseline periods (50–650 ms) in phasic REM, tonic REM, and wakefulness. Statistical parameters (*T* value) of within-state comparisons along the time × frequency axis are highlighted. *B*, significant clusters at each time × frequency point after cluster-based permutation statistics are highlighted. [Colour figure can be viewed at wileyonlinelibrary.com]

of the ANT, showing distinct signatures of interoceptive processing in phasic REM compared with tonic REM and wakefulness.

Sleep in general, and especially REM sleep, has long been viewed as a state of reduced environmental alertness. However, a wide variety of studies indicate that the sleeping brain is not fully impermeable to external stimulation (Salvesen et al., 2024). Although its potential to integrate and process complex information is limited, a range of cognitive operations remains functional, allowing the sleeping brain to process or suppress external inputs (Andrillon & Kouider, 2020). Whereas cortical reactivity to external inputs in the sleeping brain were extensively studied (Bastuji & García-Larrea, 1999; Colrain, 2005; Halasz et al., 2004; Halász et al., 2014), neural responses to interoceptive signals received relatively less attention. Nonetheless, previous studies indicate that beyond exteroception (mostly studied in the auditory domain), the sleeping brain is also susceptible to interoceptive signals, which, by providing a rich source of information, seem to affect the regulation of sleep and arousal (Mazza et al., 2012; Wei & Van Someren, 2020).

Recent studies suggest that during REM sleep, the alternation between phasic and tonic periods facilitates environmental disconnection and alertness, respectively. Specifically, while the processing of auditory inputs is largely reduced in phasic REM sleep, cortical responses to external stimulation are reinstated during tonic REM periods (Koroma et al., 2020; Sallinen et al., 1996; Takahara et al., 2006, 2002; Wehrle et al., 2007). In line with studies on auditory processing, a recent study (Simor, Bogdány et al., 2021) examined HEPs of scalp electrode recordings in phasic and tonic REM sleep, and observed different modulation of HEPs at late components (∼550–650 ms) in phasic compared with tonic REM and wakefulness. Moreover, similar to results in auditory stimulation studies (Sallinen et al., 1996; Wehrle et al., 2007), HEPs in tonic REM sleep featured intermediate values between those of phasic REM and wakefulness (Simor, Bogdány et al., 2021). Our findings in the ANT align with this pattern: amplitude modulations locked to the heartbeat in the ANT differed between phasic and tonic REM during late potentials (400–600 ms) and between phasic REM and wakefulness (370–550 ms), with HEPs in tonic REM appearing intermediate between phasic REM and wakefulness. Moreover, such differences in HEPs were not confounded by differences in ECG amplitudes. Notably, HEP modulations differing across states were observed at slightly earlier time points in the current study compared with findings on the level of the scalp. Since the ANT, in coordination with other fronto-limbic regions, is involved in the integration of visceral afferents, we may speculate that signals from the visceral pathway reach the ANT before being processed in cortical layers. Likewise, heartbeat-related neural responses in deeper brain regions (e.g. insula) were observed at relatively earlier time points (Park et al., 2018) than HEPs in scalp EEG recordings (Coll et al., 2021).

Heartbeat-related phase modulations of oscillatory activity, as quantified by ITPC, revealed a robust increase in phase alignment at lower frequencies (7–20 Hz) during REM states and wakefulness. This finding aligns with a previous study that examined ITPC of LFPs recorded intracranially from the insula (Park et al., 2018), a key region involved in interoceptive processing (Berntson & Khalsa, 2021; Chen et al., 2021; Craig & Craig, 2009; Park & Blanke, 2019; Seth, 2013). In that study, the authors observed an increase in ITPC lasting approximately 400 ms after the R-peak during resting wakefulness and during conditions that enhance interoceptive processing (Park et al., 2018). Our findings corroborate this result by demonstrating strikingly similar increases in ITPC with respect to both temporal and frequency characteristics. Moreover, our finding indicates that oscillatory activity in the ANT seems to track cardiac signals not only in wakefulness, but also in REM sleep. While phase alignment in lower frequencies was not distinct between the three vigilance states, beta–low gamma power was relatively reduced in phasic REM compared with tonic REM and resting wakefulness. The reduction of heartbeat-related beta–low gamma power was paralleled by a decrease in gamma synchronization (ITPC) apparent only in phasic REM sleep. In sum, in addition to HEPs, modulations of time-frequency power and synchronization in the beta–low gamma and gamma frequency range, respectively, point to distinct processing of cardiac signals in the ANT during the phasic REM state.

Although the specific role of heartbeat-related activity in the ANT in interoception should be explored in future studies that experimentally manipulate interoceptive processing, our findings offer new insights into the distinctive nature of phasic REM sleep. Building on previous studies that primarily investigated the exteroceptive (predominantly acoustic) domain, we found that neural activity associated with cardiac events differs in phasic REM compared with tonic REM and wakefulness. Additionally, consistent with prior research on evoked and spontaneous neural activity (Andrillon & Kouider, 2020; Koroma et al., 2020; Simor et al., 2020), our findings place tonic REM sleep as an intermediate state between phasic REM and resting wakefulness. Although the present findings only evidence the distinctiveness of cardiac-related anterior thalamic activity in phasic REM, we may speculate that such indices point to the reduction of interoceptive processing in phasic REM sleep. More specifically, we propose that reduced high-frequency power and synchronization in response to heartbeats may reflect attenuated processing of interoceptive afferents during phasic REM periods. Beta EEG oscillations are commonly implicated in sensorimotor processing

(Pfurtscheller & Da Silva, 1999). Recent evidence suggests that beta EEG waves are inherently transient in nature, whereas distinct types of beta bursts have different functions (Lundqvist et al., 2024). Indeed, according to current insights into the functional role of these oscillatory bursts, decreased beta activity in the period after the ECG R-peak in phasic REM sleep could indicate blunted interareal communication (Lundqvist et al., 2024), which might arise shortly after the interoceptive input. In addition, gamma band activity is associated with cortical information processing, modulating attention and awareness (Fell et al., 2003; Kaiser & Lutzenberger, 2003), and enhancing the neural gain of exteroceptive (van Es & Schoffelen, 2019) and interoceptive inputs (Li et al., 2023). For instance, induced changes (increases) in gamma band power were linked to selective attention to nociceptive stimuli (Tiemann et al., 2010) and to the subjective intensity of pain (Zhang et al., 2012). Phasic REM sleep is viewed as a closed-loop state in which the influence of (bottom-up) lower-level signals arising from the sensory periphery is largely reduced (Simor et al., 2020; Wehrle et al., 2007). From the perspective of predictive coding, attenuated processing of sensory inputs from the periphery is thought to contribute to the fragmented, discontinuous, and vague nature of dreams. In the absence of constraints provided by prediction errors from sensory inputs, the brain transitions from one prediction to another, resulting in the bizarre and uncertain perceptual experiences characteristic of dreaming (Bucci & Grasso, 2017). A rare exception is the state of lucid dreaming, a unique experience that typically occurs during phasic REM sleep (Baird et al., 2022, 2019; Simor et al., 2022). In this state, the processing of lower-level signals – particularly vestibular, proprioceptive and interoceptive bodily signals – is assumed to be enhanced and transmitted to the brain's multimodal, associative processing levels (Simor et al., 2022). The attenuation of cardiac signals in phasic REM sleep might be associated with reduced neural gain on lower-level afferent pathways. This diminished neural gain on interoceptive signals is consistent with the particularly unstable nature of autonomic nervous system activity during phasic REM sleep, characterized by irregular breathing, sudden surges in heart rate and blood pressure, and impaired thermoregulation (Amici & Zoccoli, 2021). Accordingly, even autonomic reflexes that facilitate homeostatic adjustments, such as the baroreflex, have been observed to be suppressed by central commands during the phasic period of REM sleep (Silvani, 2008; Silvani & Dampney, 2013). Attenuated sampling (and information processing) of the sensory periphery during periods of phasic REM sleep is paralleled by increased activity in a thalamocortical network which seems to operate in isolation from the inputs of the external environment (Maquet et al., 1996; Miyauchi et al., 2009; Wehrle et al., 2007). Although the functions of such internally driven processing remain elusive, recent animal studies suggest that saccades of REMs are associated with the internal representation of a virtual environment (i.e. the generative model of the real world) in which the animal simulates actions and sensory outcomes (Senzai & Scanziani, 2024, 2022), which may give rise to perceptually immersive dreams.

Acknowledging the limitations of the present study, we note that due to the small sample size, our findings should be interpreted with caution. Further research is needed to determine whether distinct heartbeat-related responses in phasic REM are present in other cortical regions involved in interoception (e.g. the insula and somatosensory cortex). Additionally, sleep recordings were conducted after surgery, leading to fragmented sleep and reduced REM sleep in our sample. Therefore, we cannot fully rule out the possibility that the medical environment affected sleep quality and interoceptive processes. Finally, the patients were on anti-seizure medication, which may have influenced oscillatory activity. Although we carefully discarded sleep periods with inter-ictal spikes or signs of pathological activities, we should be cautious in generalizing our findings. Future studies applying DBS in non-epileptic clinical conditions may explore heartbeat-related neural activity in other subcortical sites.

Understanding the characteristics of REM microstates could also be relevant from a clinical point of view. For instance, patients with refractory epilepsy compared with patients with less severe, medically controlled epilepsy showed a reduction in phasic REM sleep (Yeh et al., 2023), in line with the observation that phasic REM seems to exert an inhibitory influence on epileptic activity by suppressing the propagation of inter-ictal spikes and pathological high-frequency oscillations (Nobili et al., 2024). Beyond epilepsy, studying the distinct nature of phasic and tonic REM sleep may also facilitate the understanding of the pathological mechanisms of other neurological conditions in which REM sleep is heavily affected. For instance, REM sleep behaviour disorder (RBD) is now recognized as a precocious expression of an alpha synucleinopathy which in 50–80% of the cases leads to severe neurodegeneration, most commonly Parkinson's disease (Howell & Schenck, 2015; Mahowald & Schenck, 2010). In RBD patients, muscle atonia during REM sleep is dysfunctional, leading to complex motor behaviours during REM sleep (Högl et al., 2022). Interestingly, these episodes occur most frequently in phasic REM, indicating abnormal motor cortex activation specifically in the phasic REM state (Manni et al., 2009). Notably, the motor behaviours observed in RBD are closely tied to the patients' dream experiences. These behaviours appear to be unconstrained by the external environment, instead

reflecting the internal mental models of the sleeper, which operate in isolation – in line with the concept of the closed-loop state characteristic of phasic REM sleep. Accordingly, cortical activity between phasic and tonic REM sleep showed more pronounced differences in RBD patients compared with controls (Sunwoo et al., 2019). In addition to neurological disorders, several mental health problems, such as post-traumatic stress disorder (de Boer et al., 2020), depression (Yasugaki et al., 2023) or insomnia (Riemann et al., 2022) also exhibit altered REM sleep and REM sleep microstructure. Exploring the neurophysiological features of the phasic and tonic constituents of REM sleep may also shed light on the pathological mechanisms of these disorders.

In summary, despite the limitations of our small clinical sample, this study provided a unique opportunity to investigate heartbeat-related activity in the anterior thalamus. Our findings contribute novel empirical evidence to the understanding of REM sleep heterogeneity, emphasizing the distinct cognitive processes that occur during phasic REM periods, particularly in relation to interoception.

References

Amici, R., & Zoccoli, G. (2021). Physiological changes in the autonomic nervous system during sleep. In: S. Chokroverty & P. Cortelli (Eds.), *Autonomic Nervous System and Sleep* (pp. 43–50). Springer International Publishing, Cham. https://doi.org/10.1007/978-3-030-62263-3_5

Andrillon, T., & Kouider, S. (2020). The vigilant sleeper: Neural mechanisms of sensory (de)coupling during sleep. *Current Opinion in Physiology, Physiology of Sleep*, **15**, 47–59.

Baird, B., Mota-Rolim, S. A., & Dresler, M. (2019). The cognitive neuroscience of lucid dreaming. *Neuroscience & Biobehavioral Reviews*, **100**, 305–323.

Baird, B., Tononi, G., & LaBerge, S. (2022). Lucid dreaming occurs in activated rapid eye movement sleep, not a mixture of sleep and wakefulness. *Sleep*, **45**(4), zsab294.

Bastuji, H., & García-Larrea, L. (1999). Evoked potentials as a tool for the investigation of human sleep. *Sleep Medicine Reviews*, **3**(1), 23–45.

Bastuji, H., Perchet, C., Legrain, V., Montes, C., & Garcia-Larrea, L. (2008). Laser evoked responses to painful stimulation persist during sleep and predict subsequent arousals. *PAIN®*, **137**(3), 589–599.

Berntson, G. G., & Khalsa, S. S. (2021). Neural circuits of interoception. *Trends in Neurosciences*, **44**(1), 17–28.

Berry, R. B., Budhiraja, R., Gottlieb, D. J., Gozal, D., Iber, C., Kapur, V. K., Marcus, C. L., Mehra, R., Parthasarathy, S., & Quan, S. F. (2012). Rules for scoring respiratory events in sleep: update of the 2007 AASM manual for the scoring of sleep and associated events: Deliberations of the sleep apnea definitions task force of the American Academy of Sleep Medicine. *Journal of Clinical Sleep Medicine*, **08**(05), 597–619.

Blumberg, M. S., Dooley, J. C., & Tiriac, A. (2022). Sleep, plasticity, and sensory neurodevelopment. *Neuron*, **110**(20), 3230–3242.

Blumberg, M. S., Lesku, J. A., Libourel, P.-A., Schmidt, M. H., & Rattenborg, N. C. (2020). What is REM sleep?. *Current Biology*, **30**(1), R38–R49.

Boccia, M., Teghil, A., Raimo, S., Di Vita, A., Grossi, D., Guariglia, C., & Palermo, L. (2023). Neural substrates of interoceptive sensibility: An integrated study in normal and pathological functioning. *Neuropsychologia*, **183**, 108504.

Bucci, A., & Grasso, M. (2017). Sleep and dreaming in the predictive processing framework.

Bueno-Junior, L. S., Ruckstuhl, M. S., Lim, M. M., & Watson, B. O. (2023). The temporal structure of REM sleep shows minute-scale fluctuations across brain and body in mice and humans. *Proceedings National Academy of Science USA*, **120**(18), e2213438120.

Chen, W. G., Schloesser, D., Arensdorf, A. M., Simmons, J. M., Cui, C., Valentino, R., Gnadt, J. W., Nielsen, L., Hillaire-Clarke, C. S., & Spruance, V. (2021). The emerging science of interoception: Sensing, integrating, interpreting, and regulating signals within the self. *Trends in Neurosciences*, **44**(1), 3–16.

Child, N. D., & Benarroch, E. E. (2013). Anterior nucleus of the thalamus: Functional organization and clinical implications. *Neurology*, **81**(21), 1869–1876.

Cohen, M. X. (2014). *Analyzing Neural Time Series Data: Theory and Practice*. The MIT Press.

Coll, M.-P., Hobson, H., Bird, G., & Murphy, J. (2021). Systematic review and meta-analysis of the relationship between the heartbeat-evoked potential and interoception. *Neuroscience & Biobehavioral Reviews*, **122**, 190–200.

Colrain, I. M. (2005). The K-complex: A 7-decade history. *Sleep*, **28**(2), 255–273.

Craig, A. D., & Craig, A. D. (2009). How do you feel–now? The anterior insula and human awareness. *Nature Reviews Neuroscience*, **10**(1), 59–70.

de Boer, M., Nijdam, M. J., Jongedijk, R. A., Bangel, K. A., Olff, M., Hofman, W. F., & Talamini, L. M. (2020). The spectral fingerprint of sleep problems in post-traumatic stress disorder. *Sleep*, **43**(4), zsz269.

Ermis, U., Krakow, K., & Voss, U. (2010). Arousal thresholds during human tonic and phasic REM sleep. *Journal of Sleep Research*, **19**(3), 400–406.

Feldman, M. J., Bliss-Moreau, E., & Lindquist, K. A. (2024). The neurobiology of interoception and affect. *Trends in Cognitive Sciences*, **28**(7), 643–661.

Fell, J., Fernández, G., Klaver, P., Elger, C. E., & Fries, P. (2003). Is synchronized neuronal gamma activity relevant for selective attention?. *Brain Research Reviews*, **42**(3), 265–272.

Fernández-Mendoza, J., Lozano, B., Seijo, F., Santamarta-Liébana, E., José Ramos-Platón, M., Vela-Bueno, A., & Fernández-González, F. (2009). Evidence of subthalamic PGO-like waves during REM sleep in humans: A deep brain polysomnographic study. *Sleep*, **32**(9), 1117–1126.

García-Cordero, I., Esteves, S., Mikulan, E. P., Hesse, E., Baglivo, F. H., Silva, W., García, M. del C., Vaucheret, E., Ciraolo, C., García, H. S., Adolfi, F., Pietto, M., Herrera, E., Legaz, A., Manes, F., García, A. M., Sigman, M., Bekinschtein, T. A., Ibáñez, A., & Sedeño, L. (2017). Attention, in and out: scalp-level and intracranial EEG correlates of interoception and exteroception. *Frontiers in Neuroscience*, **11**, 411.

Gonzalo-Ruiz, A., Sanz-Anquela, M. J., & Lieberman, A. R. (1995). Cholinergic projections to the anterior thalamic nuclei in the rat: A combined retrograde tracing and choline acetyl transferase immunohistochemical study. *Anatomy and Embryology*, **192**(4), 335–349.

Grodd, W., Kumar, V. J., Schüz, A., Lindig, T., & Scheffler, K. (2020). The anterior and medial thalamic nuclei and the human limbic system: Tracing the structural connectivity using diffusion-weighted imaging. *Scientific Reports*, **10**(1), 10957.

Halász, P., Bódizs, R., Parrino, L., & Terzano, M. (2014). Two features of sleep slow waves: Homeostatic and reactive aspects–from long term to instant sleep homeostasis. *Sleep Medicine*, **15**(10), 1184–1195.

Halasz, P., Terzano, M., Parrino, L., & Bodizs, R. (2004). The nature of arousal in sleep. *Journal of Sleep Research*, **13**(1), 1–23.

Hasegawa, E., Miyasaka, A., Sakurai, K., Cherasse, Y., Li, Y., & Sakurai, T. (2022). Rapid eye movement sleep is initiated by basolateral amygdala dopamine signaling in mice. *Science*, **375**(6584), 994–1000.

Högl, B., Arnulf, I., Bergmann, M., Cesari, M., Gan-Or, Z., Heidbreder, A., Iranzo, A., Krohn, L., Luppi, P., Mollenhauer, B., Provini, F., Santamaria, J., Trenkwalder, C., Videnovic, A., & Stefani, A. (2022). Rapid eye movement sleep behaviour disorder: Past, present, and future. *Journal of Sleep Research*, **31**(4), e13612.

Hong, J., Lozano, D. E., Beier, K. T., Chung, S., & Weber, F. (2023). Prefrontal cortical regulation of REM sleep. *Nature Neuroscience*, **26**(10), 1820–1832.

Howell, M. J., & Schenck, C. H. (2015). Rapid eye movement sleep behavior disorder and neurodegenerative disease. *Journal of the American Medical Association Neurology*, **72**(6), 707.

Immanuel, S. A., Pamula, Y., Kohler, M., Martin, J., Kennedy, D., Nalivaiko, E., Saint, D. A., & Baumert, M. (2014). Heartbeat evoked potentials during sleep and daytime behavior in children with sleep-disordered breathing. *American Journal of Respiratory and Critical Care Medicine*, **190**(10), 1149–1157.

Jouvet, M. (1965). Paradoxical sleep—A study of its nature and mechanisms. *Progress in Brain Research*, **18**, 20–62.

Kaiser, J., & Lutzenberger, W. (2003). Induced gamma-band activity and human brain function. *The Neuroscientist*, **9**(6), 475–484.

Keil, A., Debener, S., Gratton, G., Junghöfer, M., Kappenman, E. S., Luck, S. J., Luu, P., Miller, G. A., & Yee, C. M. (2014). Committee report: Publication guidelines and recommendations for studies using electroencephalography and magnetoencephalography. *Psychophysiology*, **51**(1), 1–21.

Koroma, M., Lacaux, C., Andrillon, T., Legendre, G., Léger, D., & Kouider, S. (2020). Sleepers selectively suppress informative inputs during rapid eye movements. *Current Biology*, **30**(12), 2411–2417.e3.

Li, W., Ma, L., Yang, G., & Gan, W.-B. (2017). REM sleep selectively prunes and maintains new synapses in development and learning. *Nature Neuroscience*, **20**,3, 427–437.

Li, Z., Zhang, L., Zeng, Y., Zhao, Q., & Hu, L. (2023). Gamma-band oscillations of pain and nociception: A systematic review and meta-analysis of human and rodent studies. *Neuroscience & Biobehavioral Reviews*, **146**, 105062.

Lőrincz, K., Bóné, B., Karádi, K., Kis-Jakab, G., Tóth, N., Halász, L., Erőss, L., Balás, I., Faludi, B., Jordán, Z., Chadaide, Z., Gyimesi, C., Fabó, D., & Janszky, J. (2023). Effects of anterior thalamic nucleus DBS on interictal heart rate variability in patients with refractory epilepsy. *Clinical Neurophysiology*, **147**, 17–30.

Lundqvist, M., Miller, E. K., Nordmark, J., Liljefors, J., & Herman, P. (2024). Beta: Bursts of cognition. *Trends in Cognitive Sciences*, **28**(7), 662–676.

Luppi, P.-H., Clément, O., Sapin, E., Gervasoni, D., Peyron, C., Léger, L., Salvert, D., & Fort, P. (2011). The neuronal network responsible for paradoxical sleep and its dysfunctions causing narcolepsy and rapid eye movement (REM) behavior disorder. *Sleep Medicine Reviews*, **15**(3), 153–163.

Mahowald, M. W., & Schenck, C. H. (2010). REM sleep parasomnias, in: *Principles and Practice of Sleep Medicine: Fifth Edition*. Elsevier Inc., pp. 1083–1097.

Manni, R., Terzaghi, M., & Glorioso, M. (2009). Motor-behavioral episodes in REM sleep behavior disorder and phasic events during REM sleep. *Sleep*, **32**(2), 241–245.

Manzano, G. M., Ragazzo, P. C., Tavares, S. M., & Marino Jr, R. (1986). Anterior zygomatic electrodes: A special electrode for the study of temporal lobe epilepsy. *Stereotactic and Functional Neurosurgery*, **49**(4), 213–217.

Maquet, P., Péters, J.-M., Aerts, J., Delfiore, G., Degueldre, C., Luxen, A., & Franck, G. (1996). Functional neuroanatomy of human rapid-eye-movement sleep and dreaming. *Nature*, **383**(6596), 163–166.

Maris, E., & Oostenveld, R. (2007). Nonparametric statistical testing of EEG- and MEG-data. *Journal of Neuroscience Methods*, **164**(1), 177–190.

Mazza, S., Magnin, M., & Bastuji, H. (2012). Pain and sleep: From reaction to action. *Neurophysiologie Clinique/Clinical Neurophysiology*, **42**(5), 337–344.

Miyauchi, S., Misaki, M., Kan, S., Fukunaga, T., & Koike, T. (2009). Human brain activity time-locked to rapid eye movements during REM sleep. *Experimental Brain Research*, **192**(4), 657–667.

Nobili, L., Cordani, R., Arnaldi, D., Mattioli, P., Veneruso, M., & Ng, M. (2024). Rapid eye movement sleep and epilepsy: Exploring interactions and therapeutic prospects. *Journal of Sleep Research*, e14251.

Oostenveld, R., Fries, P., Maris, E., & Schoffelen, J.-M. (2011). FieldTrip: Open source software for advanced analysis of MEG, EEG, and invasive electrophysiological data. *Computational Intelligence and Neuroscience*, **2011**, 1–9.

Park, H.-D., Bernasconi, F., Salomon, R., Tallon-Baudry, C., Spinelli, L., Seeck, M., Schaller, K., & Blanke, O. (2018). Neural sources and underlying mechanisms of neural responses to heartbeats, and their role in bodily self-consciousness: An intracranial EEG study. *Cerebral Cortex*, **28**(7), 2351–2364.

Park, H.-D., & Blanke, O. (2019). Heartbeat-evoked cortical responses: Underlying mechanisms, functional roles, and methodological considerations. *Neuroimage*, **197**, 502–511.

Perakakis, P. (2019). HEPLAB: A Matlab graphical interface for the preprocessing of the heartbeat-evoked potential. *Zenodo*.

Perogamvros, L., Park, H.-D., Bayer, L., Perrault, A.A., Blanke, O., & Schwartz, S. (2019). Increased heartbeat-evoked potential during REM sleep in nightmare disorder. *NeuroImage: Clinical*, **22**, 101701.

Pfurtscheller, G., & daSilva, F. L. (1999). Event-related EEG/MEG synchronization and desynchronization: Basic principles. *Clinical Neurophysiology*, **110**(11), 1842–1857.

Pollatos, O., Schandry, R., Auer, D. P., & Kaufmann, C. (2007). Brain structures mediating cardiovascular arousal and interoceptive awareness. *Brain Research*, **1141**, 178–187.

Riemann, D., Benz, F., Dressle, R. J., Espie, C. A., Johann, A. F., Blanken, T. F., Leersen, J., Wassing, R., Henry, A. L., Kyle, S. D., Spiegelhalder, K., & Van Someren, E. J. (2022). Insomnia disorder: State of the science and challenges for the future. *Journal of Sleep Research*, **31**(4), e13604.

Sallinen, M., Kaartinen, J., & Lyytinen, H. (1996). Processing of auditory stimuli during tonic and phasic periods of REM sleep as revealed by event-related brain potentials. *Journal of Sleep Research*, **5**(4), 220–228.

Salvesen, L., Capriglia, E., Dresler, M., & Bernardi, G. (2024). Influencing dreams through sensory stimulation: A systematic review. *Sleep Medicine Reviews*, **74**, 101908.

Schandry, R., Sparrer, B., & Weitkunat, R. (1986). From the heart to the brain: A study of heartbeat contingent scalp potentials. *International Journal of Neuroscience*, **30**(4), 261–275.

Senzai, Y., & Scanziani, M. (2024). The brain simulates actions and their consequences during REM sleep. *bioRxiv*. https://doi.org/10.1101/2024.08.13.607810

Senzai, Y., & Scanziani, M. (2022). A cognitive process occurring during sleep is revealed by rapid eye movements. *Science*, **377**(6609), 999–1004.

Seth, A. K. (2013). Interoceptive inference, emotion, and the embodied self. *Trends in Cognitive Sciences*, **17**(11), 565–573.

Silvani, A. (2008). Physiological sleep-dependent changes in arterial blood pressure: Central autonomic commands and baroreflex control. *Clinical and Experimental Pharmacology & Physiology*, **35**(9), 987–994.

Silvani, A., & Dampney, R. A. L. (2013). Central control of cardiovascular function during sleep. *American Journal of Physiology-Heart and Circulatory Physiology*, **305**(12), H1683–H1692.

Simor, P., Bogdány, T., Bódizs, R., & Perakakis, P. (2021). Cortical monitoring of cardiac activity during rapid eye movement sleep: The heartbeat evoked potential in phasic and tonic rapid-eye-movement microstates. *Sleep*, **44**(9), zsab100.

Simor, P., Bogdány, T., & Peigneux, P. (2022). Predictive coding, multisensory integration, and attentional control: A multicomponent framework for lucid dreaming. *Proceedings of the National Academy of Sciences*, **119**(44), e2123418119.

Simor, P., Szalárdy, O., Gombos, F., Ujma, P. P., Jordán, Z., Halász, L., Erőss, L., Fabó, D., & Bódizs, R. (2021). REM sleep microstates in the Human anterior thalamus. *Journal of Neuroscience*, **41**(26), 5677–5686.

Simor, P., van der Wijk, G., Nobili, L., & Peigneux, P. (2020). The microstructure of REM sleep: Why phasic and tonic?. *Sleep Medicine Reviews*, **52**, 101305.

Suarez, M., Maglianesi, M. A., & Perassi, N. I. (1998). Involvement of the anterodorsal thalami nuclei on the hypophysoadrenal response to chronic stress in rats. *Physiology & Behavior*, **64**, 111–116.

Sunwoo, J.-S., Cha, K.S., Byun, J.-I., Kim, T.-J., Jun, J.-S., Lim, J.-A., Lee, S.-T., Jung, K.-H., Park, K.-I., Chu, K., Kim, H.-J., Kim, M., Lee, S. K., Kim, K. H., Schenck, C. H., & Jung, K.-Y. (2019). Abnormal activation of motor cortical network during phasic REM sleep in idiopathic REM sleep behavior disorder. *Sleep*, **42**(2).

Szalárdy, O., Simor, P., Ujma, P. P., Jordán, Z., Halász, L., Erőss, L., Fabó, D., & Bódizs, R. (2024). Temporal association between sleep spindles and ripples in the human anterior and mediodorsal thalamus. *European Journal of Neuroscience*, **59**(4), 641–661.

Takahara, M., Nittono, H., & Hori, T. (2006). Effect of voluntary attention on auditory processing during REM sleep. *Sleep*, **29**, 975–982.

Takahara, M., Nittono, H., & Hori, T. (2002). Comparison of the event-related potentials between tonic and phasic periods of rapid eye movement sleep. *Psychiatry and clinical neurosciences*, **56**(3), 257–258.

Team. (2020), J., 2020. JASP (Version 0.14. 1)[Computer Software].

Tiemann, L., Schulz, E., Gross, J., & Ploner, M. (2010). Gamma oscillations as a neuronal correlate of the attentional effects of pain. *Pain*, **150**(2), 302–308.

van Es, M. W. J., & Schoffelen, J.-M. (2019). Stimulus-induced gamma power predicts the amplitude of the subsequent visual evoked response. *Neuroimage*, **186**, 703–712.

Vertes, R. P., Albo, Z., & di Prisco, G. V. (2001). Theta-rhythmically firing neurons in the anterior thalamus: Implications for mnemonic functions of Papez's circuit. *Neuroscience*, **104**(3), 619–625.

Wehrle, R., Kaufmann, C., Wetter, T. C., Holsboer, F., Auer, D. P., Pollmächer, T., & Czisch, M. (2007). Functional microstates within human REM sleep: First evidence from fMRI of a thalamocortical network specific for phasic REM periods. *European Journal of Neuroscience*, **25**(3), 863–871.

Wei, Y., & van Someren, E. J. (2020). Interoception relates to sleep and sleep disorders. *Current Opinion in Behavioral Sciences*, **33**, 1–7.

Yasugaki, S., Okamura, H., Kaneko, A., & Hayashi, Y. (2023). Bidirectional relationship between sleep and depression. *Neuroscience Research*, **211**, 57–64.

Yeh, W.-C., Li, Y.-S., & Hsu, C.-Y. (2023). Reduction in the propensity of rapid eye movement sleep and phasic-to-tonic ratio in patients with refractory epilepsy. *Sleep*, **46**(7), zsad115.

Zhang, Z.G., Hu, L., Hung, Y. S., Mouraux, A., & Iannetti, G. D. (2012). Gamma-band oscillations in the primary somatosensory cortex—A direct and obligatory correlate of subjective pain intensity. *Journal of Neuroscience*, **32**(22), 7429–7438.

Additional information

Data availability statement

All scripts used for the analyses as well as the preprocessed data are available at https://github.com/rokazita/ANT-REM-HEP.

Competing interests

No competing interests declared.

Author contributions

R.B.: Conception or design of the work; Acquisition, analysis or interpretation of data for the work; Drafting the work or revising it critically for important intellectual content; Final approval of the version to be published; Agreement to be accountable for all aspects of the work. Z.L.R.: Conception or design of the work; Acquisition, analysis or interpretation of data for the work; Drafting the work or revising it critically for important intellectual content; Final approval of the version to be published; Agreement to be accountable for all aspects of the work. O.S.: Conception or design of the work; Acquisition, analysis or interpretation of data for the work; Drafting the work or revising it critically for important intellectual content; Final approval of the version to be published; Agreement to be accountable for all aspects of the work. Z.J.: Conception or design of the work; Acquisition, analysis or interpretation of data for the work; Drafting the work or revising it critically for important intellectual content; Final approval of the version to be published; Agreement to be accountable for all aspects of the work. L.H.: Conception or design of the work; Acquisition, analysis or interpretation of data for the work; Drafting the work or revising it critically for important intellectual content; Final approval of the version to be published; Agreement to be accountable for all aspects of the work. L.E.: Conception or design of the work; Acquisition, analysis or interpretation of data for the work; Drafting the work or revising it critically for important intellectual content; Final approval of the version to be published; Agreement to be accountable for all aspects of the work. D.F.: Conception or design of the work; Acquisition, analysis or interpretation of data for the work; Drafting the work or revising it critically for important intellectual content; Final approval of the version to be published; Agreement to be accountable for all aspects of the work. P.S.: Conception or design of the work; Acquisition, analysis or interpretation of data for the work; Drafting the work or revising it critically for important intellectual content; Final approval of the version to be published; Agreement to be accountable for all aspects of the work.

Funding

National Research, Development and Innovation Office: Róbert Bódizs, Orsolya Szalárdy, Zsófia Jordán, Loránd Erőss, Dániel Fabó, K_128 117; Ministry of Innovation and Technology: Róbert Bódizs, TKP2021-EGA-25; Ministry of Innovation and Technology: Róbert Bódizs, TKP2021-NKTA-47; Magyar Tudományos Akadémia (MTA): Péter Simor, János Bolyai; Innovációs és Technológiai Minisztérium (Ministry for Innovation and Technology): Zita Lilla Róka, ÚNKP-23-1.

Acknowledgements

The work was supported by the National Research, Development and Innovation Office of Hungary K_128117 (RB), FK 142945 (PS) and by the Ministry of Innovation and Technology of Hungary (TKP2021-EGA-25, TKP2021-NKTA-47). PS received the János Bolyai scholarship of the Hungarian Academy of Sciences. ZR was supported by the ÚNKP-23-1 New National Excellence Program of the Ministry for Innovation and Technology from the source of the National Research, Development and Innovation Fund.

Keywords

anterior thalamic nucleus, heartbeat, interoception, REM sleep, thalamography

Supporting information

Additional supporting information can be found online in the Supporting Information section at the end of the HTML view of the article. Supporting information files available:

Peer Review History